*Biochimica et Biophysica Acta*, 1020 (1990) 239–246
Elsevier

BBABIO 43284

# Charge transfer and charge resonance states of the primary electron donor in wild-type and mutant bacterial reaction centers

Lynda M. McDowell, Christine Kirmaier and Dewey Holten

*Department of Chemistry, Washington University, St. Louis, MO (U.S.A.)*

(Received 15 March 1990)
(Revised manuscript received 9 July 1990)

Key words: Reaction center; Charge transfer; Bacteriopheophytin; Bacteriochlorophyll; Electron transfer; Transient state

**Low-temperature subpicosecond measurements on heterodimer-containing reaction centers from the His$^{M200}$ → Leu mutant of *Rhodobacter capsulatus* are reported. As at room temperature, primary electron transfer is initiated from a state of the bacteriochlorophyll (BChl)/bacteriopheophytin (BPh) heterodimer with substantial [BChl$^+$BPh$^-$] intradimer charge transfer character. The electronic composition of this transient state is discussed in terms of mixing of the exciton and charge resonance states of the BChl/BPh dimer and compared with the nature of the excited states of the BChl/BChl dimer in wild-type reaction centers.**

## Introduction

Much recent work on bacterial photosynthetic reaction centers (RCs) has focused on a detailed description of the electronic nature of the excited primary electron donor (P*), and consequent influences on both the optical properties of P and the rapid, unidirectional electron transfer from P* to the L-side bacteriopheophytin molecule (BPh$_L$). (P is a dimer of bacteriochlorophyll (BChl) molecules. The L and M subscripts refer to the polypeptide with which the cofactor is most closely associated [1–3].) Widespread attention has been given to the idea that P* derives charge transfer (CT) character via coupling between the (BChl)$_2$ exciton states and internal (intradimer) CT states (e.g., [BChl$^+_{LP}$ BChl$^-_{MP}$]). CT character in P* is thought to be important in determining the position and width of the long-wavelength ground state absorption band of P [4–6], the hole-burning [7–10] and Stark effect [11–13] spectra of this band, the magnetic properties of the dimer triplet state [14–16], and the directionality and mechanism of the initial electron transfer reaction [4,6,17–20]. One difficulty in evaluating these proposals is a lack of direct information on the energies of the intradimer CT states and how they couple with each other and the exciton states of P.

RCs from the His$^{M200}$ → Leu mutant of *Rhodobacter (Rb.) capsulatus* have provided an important vehicle for examining the photophysical behavior of intradimer CT states [21–25]. This mutant contains a BChl$_{LP}$/BPh$_{MP}$ heterodimer (which has been called D, for donor) in place of the BChl$_{LP}$/BChl$_{MP}$ dimeric primary donor in wild-type RCs [21]. Recent room-temperature subpicosecond transient absorption studies on this mutant have revealed an anion band centered near 650 nm in the 0.6 ps spectrum; no such feature is seen in the P* spectrum of wild-type RCs. On the basis of this spectrum, photodichroism measurements, and energetic considerations, it was suggested that the state observed immediately (< 350 fs) after excitation of the heterodimer is basically the intradimer CT state [BChl$^+_{LP}$BPh$^-_{MP}$] [23]. This initially observed transient state was found to have a lifetime of about 15 ps at room temperature and to decay via two pathways: electron transfer to the normal BPh$_L$ acceptor and rapid internal conversion (charge recombination) to the ground state, both with a yield of about 50% [22,23]. (By comparison, the P* lifetime in wild-type RCs is about 3 ps and the yield of electron transfer to BPh$_L$ is near unity [26].) We report here that this anion-bearing transient state is also the initially observed state in His$^{M200}$ → Leu RCs at 77 K. The results on the mutant permit us to estimate the energy of the state in wild-type RCs from which P* derives its CT character and to discuss the electronic composition of the excited primary donor in both wild-type and heterodimer-containing RCs.

---

Correspondence: D. Holten, Department of Chemistry, Washington University, St. Louis, MO 63130-4899, U.S.A.

0005-2728/90/$03.50

## Experimental

Wild-type RCs from *Rb. capsulatus* U43(L228BamHI) [21] and His$^{M200}$ → Leu RCs were prepared as described [27], except that the chromatophores were diluted to $A_{875} = 24$ (1 cm pathlength) before the detergent extraction. The RCs were studied in either poly(vinyl alcohol) films or 60% glycerol/buffer glasses. Samples typically had ground state absorptions of $A_{798} = 4.0$ (mutant) and $A_{802} = 2.6$ (wild-type) at room temperature. Subpicosecond transient absorption measurements were performed as previously described, and utilized either 15 μJ 150 fs 870 nm or 50 μJ 350 fs 582 nm excitation flashes polarized at 45° with respect to the white-light probe pulses [22,23]. The excitation flashes were focused to 1–2 mm at the sample and typically excited 20–40% of the RCs. Temperature control was provided by an Oxford Instruments DN1704 optical cryostat system. Each spectrum shown in Figs. 1 and 4 are the average of about 300 spectra and have a typical standard deviation in $\Delta A$ of 0.005.

## Results

Fig. 1 shows the transient absorption spectrum observed immediately after subpicosecond excitation of His$^{M200}$ → Leu RCs at 77 K (solid spectrum at 0.3 ps). Characteristic features of this spectrum include bleaching of the long-wavelength (840–920 nm) absorption of the heterodimer (inset), bleaching in the BPh $Q_X$ region at 548 nm, and a broad absorption band having a peak near 650 nm. This spectrum is essentially the same as previously reported at 285 K and can be assigned to a transient state having mainly [$\mathrm{BChl}_{LP}^{+}\mathrm{BPh}_{MP}^{-}$] intradimer CT character (see below and Ref. 23). The photochemistry proceeding from this state, which we denote $D^{\pm}$, is also largely unchanged at low temperature, as summarized in the simplified state diagram shown in Fig. 2. In particular, $D^{\pm}$ decays with a time constant of about 20 ps at 77 K. This decay is accompanied by spectral changes in the three key regions shown in Fig. 1: (i) A portion (50–65%) of the near-infrared heterodimer bleaching decays with a time constant of 21 ± 6 ps (kinetic data not shown), reflecting return of about half of the RCs to the ground state. (ii) The initial anion band centered at 650 nm decays with a time constant of 17 ± 5 ps (the first component of the dual-exponential decay observed in this region, Fig. 3) and is replaced by an anion band centered at 665 nm (Fig. 1, dashed), which we can assign to the $\mathrm{BPh}_L^-$ absorption of state $D^+\mathrm{BPh}_L^-$. In keeping with this, the 665 nm anion band has the same peak wavelength as the $\mathrm{BPh}_L$ anion in state $P^+\mathrm{BPh}_L^-$ in wild-type RCs (Fig. 4B, dashed). (iii) The BPh $Q_X$ bleaching partially (50–60%) decays with a time constant of 18 ± 5 ps (the first component of the dual exponential decay observed in this region) as the electron moves to $\mathrm{BPh}_L$. These data combine to demonstrate that at 77 K state $D^{\pm}$ has a lifetime of about 20 ps and decays by about half to the ground state and by about half to state $D^+\mathrm{BPh}_L^-$. These results are essentially the same as those found at 285 K [22,23].

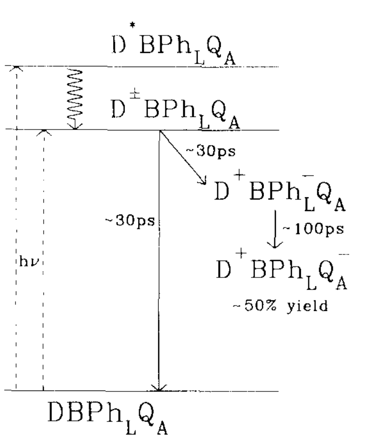

Fig. 2. Schematic state diagram for the primary photochemistry in *Rb. capsulatus* His$^{M200}$ → Leu RCs. As discussed in the text, the state labelled $D^*$ has mostly heterodimer exciton character and the state labelled $D^{\pm}$ has mainly [$\mathrm{BChl}_{LP}^{+}\mathrm{BPh}_{MP}^{-}$] intradimer CT character. Both $D^*$ and $D^{\pm}$ may contribute to the long-wavelength region of the broad near-infrared absorption of the heterodimer, as discussed in the text.

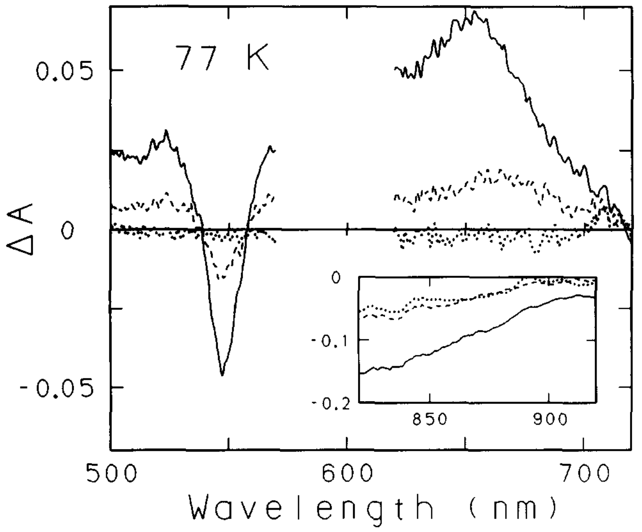

Fig. 1. Low-temperature (77 K) absorption difference spectra of His$^{M200}$ → Leu RCs at (———) 0.3 ps, (— — —) 46 ps, and (······) 2 ns after excitation with a 150 fs 870 nm flash. The inset shows the bleaching of the near-infrared absorption of D at 2.3 ps (———), 71 ps (— — —) at 0.95 ns (······) after a 582 nm flash.

Fig. 2 also shows that in a subsequent step an electron is transferred from $\mathrm{BPh}_L^-$ to $Q_A$. This is manifested by decay of the 665 nm anion band with a time constant of 60 ± 12 ps (the second phase of the dual-exponential decay in this region, Fig. 3). A similar time constant is obtained for the second component of the

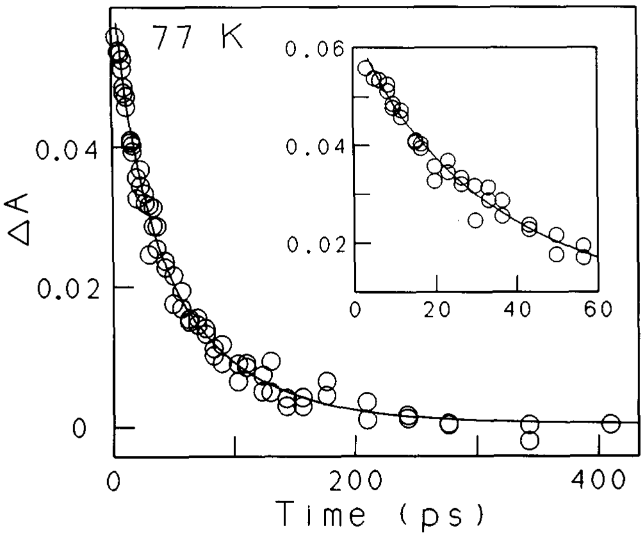

Fig. 3. Decay kinetics of the 660–670 nm transient absorption in $His^{M200} \rightarrow Leu$ RCs at 77 K following a 150 fs 870 nm excitation flash. Data points taken between 1 and 2 ns after excitation are not shown, but were included in the fits (solid line) of the data to a constant plus two exponentials. The fit yields time constants of $\tau_1 = 19 \pm 6$ ps for the decay of $D^{\pm}$ and $\tau_2 = 67 \pm 12$ ps for electron transfer from $BPh_L^-$ to $Q_A$. Averaging all values obtained in the anion band gives lifetimes of $17 \pm 5$ ps and $60 \pm 12$ ps. The inset shows an expanded view of the data at early times.

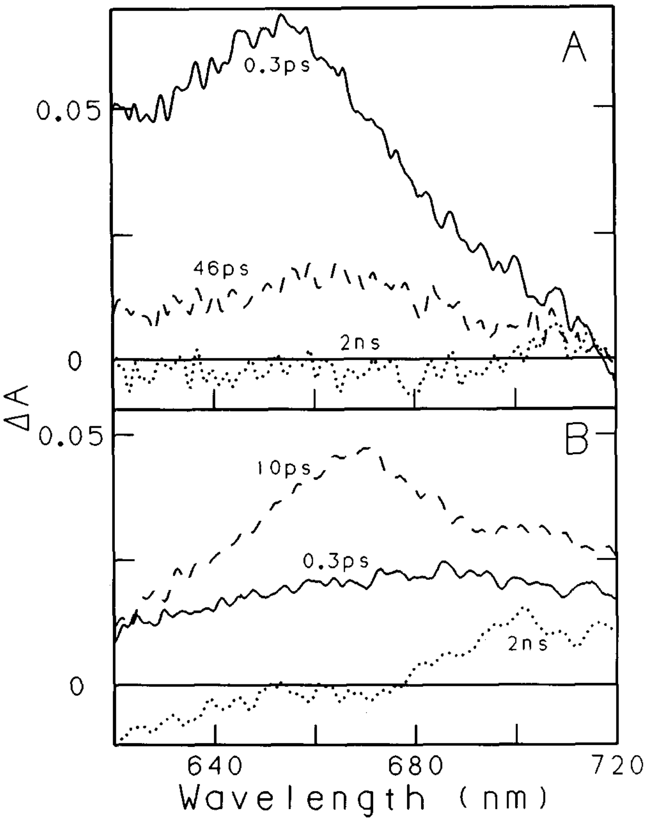

Fig. 4. Low-temperature (77 K) transient absorption difference spectra in the BPh anion absorption region acquired at several delay times after excitation with a 150 fs flash at 870 nm: (A) $His^{M200} \rightarrow Leu$ RCs and (B) wild-type RCs.

decay in the BPh $Q_X$ region. Comparison of the 71 ps (dashed) and 0.95 ns (dotted) spectra in the inset to Fig. 1 shows that no decay of the heterodimer bleaching is observed on this timescale, reflecting the same, about 100%, yield of electron transfer from $BPh_L^-$ to $Q_A$ as found at room temperature in $His^{M200} \rightarrow Leu$ RCs, and in wild-type *Rb. capsulatus* RCs [22,23]. The time constant of about 60 ps for $D^+BPh_L^- \rightarrow D^+Q_A^-$ at 77 K is slightly faster than the time constant of about 100 ps observed for this process at 285 K [22]. It is important to note that no bleaching is observed in the 530 nm $BPh_M$ $Q_X$ band at any time from 0.3 ps to 1 ns (Fig. 1). Preferential electron transfer to $BPh_L$ is thus preserved in $His^{M200} \rightarrow Leu$ RCs at low temperature.

The anion band centered near 650 nm in the 0.3 ps spectrum of $His^{M200} \rightarrow Leu$ RCs is the key to our assignment of transient state $D^{\pm}$ as having mainly $[BChl_{LP}^+BPh_{MP}^-]$ intradimer CT character (see Fig. 1 and expanded view in Fig. 4A). Such an anion band is not observed in the $P^*$ spectrum of wild-type RCs at either 77 K (0.3 ps spectrum in Fig. 4B) or 285 K [23]. Instead, the $P^*$ spectrum is featureless in this region, as expected for a state which is basically $^1(\pi, \pi^*)$ in character [28–30]. The only other anion-bearing transient state which could be associated with the 0.3 ps spectrum in $His^{M200} \rightarrow Leu$ RCs is $D^+BChl_L^-$ (or $D^+BChl_M^-$); however, other data are not consistent with formation of an anion of BChl. As discussed previously [23], $D^+BChl_L^-$ would be expected to give a prominant bleaching in the 800 nm $Q_Y$ band of $BChl_L$, which is not observed. Further evidence against state $D^+BChl_L^-$ comes from the BPh $Q_X$ region of the transient absorption spectra (Fig. 1) and two reasonable postulates: (i) the $Q_X$ bands of the two components of the heterodimer should be only weakly coupled and behave roughly as monomer-like transitions (as in porphyrin dimers [31]), and (ii) the hole in $D^+$ should be localized preferentially on the BChl half of the heterodimer (since BChl is easier to oxidize than BPh [32,33]). The absence of BPh $Q_X$ bleaching in the $D^+Q_A^-$ spectrum (Fig. 1, dotted) supports these ideas. Thus, if the initially observed transient state were $D^+BChl_L^-$, then little BPh $Q_X$ bleaching would be expected in the 0.3 ps spectrum, contrary to observation. On the other hand, such bleaching is expected for a state with substantial $[BChl_{LP}^+BPh_{MP}^-]$ intradimer CT character because the $BPh_{MP}$ component of the heterodimer is removed from the ground state.

Two independent estimates of the extinction coefficient of the 650 nm anion band in the 0.3 ps spectrum of $D^{\pm}$ indicate that it is comparable to that of the 665 nm band of $BPh_L^-$. The first estimate comes from comparative measurements at 285 K on wild-type and $His^{M200} \rightarrow Leu$ samples having the same concentration (based on the absorption band near 800 nm). Such samples also have the same absorption at 582 nm (see

Fig. 1 in Ref. 22), and when these matched samples are studied under identical experimental conditions using 582 nm excitation, the amplitude of the 650 nm anion band in the subpicosecond spectrum of His$^{M200}$ → Leu RCs is about 20% larger than the 665 nm anion band observed for $P^+BPh_L^-$ in wild-type RCs (data not shown). The second measure of the extinction coefficient at 650 nm of $D^\pm$ comes from the dual-exponential fits of the data in the anion region acquired following 870 nm flashes (Fig. 3): The two components due to $D^\pm$ and $D^+BPh_L^-$ decay (15 and 100 ps at 285 K [22] and 17 and 60 ps at 77 K), are partitioned roughly 60/40, respectively. Since $D^+BPh_L^-$ has a yield of about 50% based on the decay of the long-wavelength heterodimer bleaching (see Fig. 1 inset), this again indicates that the subpicosecond anion band in the mutant has an extinction coefficient comparable to that of the $BPh_L$ anion band. Thus, the shape and amplitude of the transient absorption in the 620–720 nm region demonstrate that upon excitation of His$^{M200}$ → Leu RCs a state ($D^\pm$) with substantial anion, and hence $[BChl_{LP}^+BPh_{MP}^-]$, character is formed in keeping with our previous analysis [23]. These results do not imply that $D^\pm$ is a pure intradimer CT state. The oxidized BChl component of D is expected to contribute some absorption in this region (but much weaker than the BPh anion) [32,33]. As discussed below, $D^\pm$ likely has some heterodimer exciton character which probably contributes a featureless absorption, as weak as in the P* spectrum of wild-type RCs.

## Discussion

The branching of the His$^{M200}$ → Leu photochemistry at the initially-observed transient state ($D^\pm$) results in a 2-fold smaller overall yield of electron transfer to $Q_A$ than is observed in wild-type RCs (Fig. 2). The (lack of) temperature dependence of the rates of both electron transfer from $D^\pm$ to $BPh_L$ and competing deactivation of $D^\pm$ to the ground state has important mechanistic implications and will be discussed elsewhere. Here we focus on (i) a discussion and comparison of the electronic composition of the excited states of D and P, (ii) the implications of ordering the ($\pi$, $\pi^*$) exciton-like state D* at higher energy than the CT-like $D^\pm$ (Fig. 2) on the interpretation of the near-infrared ground state absorption of the heterodimer, and (iii) relationships between the electronic structure of the primary electron donor and the mechanism of the initial stage(s) of charge separation in both His$^{M200}$ → Leu and wild-type RCs.

### *Excited states of the primary donor in wild-type RCs*

The lowest electronic states of P in wild-type RCs are thought to be derived mainly from mixing among four zeroth-order basis configurations, the two monomer $Q_Y$ excited configurations $BChl_{LP}^*$ and $BChl_{MP}^*$ and the two intradimer CT configurations $[BChl_{LP}^+BChl_{MP}^-]$ and $[BChl_{LP}^-BChl_{MP}^+]$. On the basis of solution redox potentials [32,33], one can obtain a rough estimate of 1.5 eV for the energy of the two intradimer CT configurations, which places them near the energy of the locally excited configurations (i.e., in the vicinity of the $Q_Y$ bands of the BChl monomers in the RC). Important, and as yet unresolved, issues are the actual energies of the two CT configurations and the extent to which they couple with the two locally excited configurations [4–6,10]. It has been customary to consider linear combinations of the two $Q_Y$ configurations, i.e., consider that they split into a higher and a lower energy exciton component. Similarly, because of the high (approx. $C_2$) symmetry of the dimer, the two intradimer CT configurations will mix substantially and split into higher and lower energy charge resonance (CR) components. (Charge resonance states are also believed to be important in determining the low energy absorption and emission properties of strongly-coupled porphyrin dimers [35]. See also note added in proof.) In this basis set it is the CR (not the CT) configurations that mix with the exciton components. If P and the surrounding protein had perfect $C_2$ symmetry (i.e., if the two CT configurations had the same energy) then the two CR components would be 50/50 mixtures of the two CT configurations, and mixing of the CR and exciton components would contribute no *net* CT character to P* (i.e., no net transfer of charge from one macrocycle of P to the other). Thus, it is possible for a state to have substantial CR character with little CT character.

Recent Stark measurements on the long-wavelength band of P have provided evidence that P* in wild-type RCs has a small net CT character. The difference in the dipole moment between P* and the ground state is found to be about 7 debye, somewhat larger than the value of about 3 D for both monomeric BChl and BPh, but much smaller than the estimated difference dipole of about 35 D for a pure intradimer CT state [11,12,20,25,36]. These measurements indicate that inherent asymmetries in the structure of P and in the surrounding protein residues result in the intradimer CT states $[BChl_{LP}^+BChl_{MP}^-]$ and $[BChl_{LP}^-BChl_{MP}^+]$ having slightly different energies and contributions to P* [5,6,11,12,19,20,25,36]. (Some calculations suggest that $[BChl_{LP}^+BChl_{MP}^-]$ may have a slightly lower energy [6,19], although the opposite viewpoint has also been expressed [5].) In other words, because of the different energies of the two opposing CT configurations, mixing of the lowest CR and exciton states will give P* net CT character. Our description of the corresponding upper excited states of P as being basically CR (not CT) states with little oscillator strength also provides an explanation for the observation that there are no prominent higher-energy Stark features [11,12,25]. That these upper states are largely CR (and not CT) states is a more fundamental explanation for the absence of higher energy Stark features than the previous suggestion that they may be too broad to be detected [5].

The conclusion from the Stark data that P* has only small intradimer CT character can be compared for consistency with the known spectrum of this state. A large body of work on porphyrins, chlorins and bacteriochlorins has shown that $^1(\pi, \pi^*)$ excited states of these molecules contain no distinct absorption bands, except in the vicinity of the ground state near-ultraviolet Soret band. At wavelengths longer than 600 nm the spectra are uniformly characterized by a weak *flat* featureless absorption [28–30]. As can be seen in Fig. 4B (0.3 ps spectrum), this description accurately applies to the P* spectrum in the key region between 620 and 720 nm, and is fully in keeping with P* having only small intradimer CT character.

*Excited states of the primary donor in His$^{M200}$ → Leu RCs*

The heterodimer obviously has much larger inherent electronic asymmetry than P. BPh is both easier to reduce and harder to oxidize than BChl by about 300 mV in vitro [32,33], meaning that the two intradimer CT configurations could be split by as much as 0.6 eV. Again, using solution redox potentials one can estimate [BChl$^+_{LP}$BPh$^-_{MP}$] to have an energy of 1.2 eV and [BChl$^-_{LP}$BPh$^+_{MP}$] an energy of 1.8 eV. The two monomer $Q_Y$ configurations BChl$^*_{LP}$ and BPh$^*_{MP}$ at 1.5–1.6 eV will lie in between. These rough estimates show that one expects substantially larger energy differences among the four basis configurations in the mutant than in wild-type RCs, particularly with respect to the CT configurations. In contrast to the case for P, the two CR states of D will *largely retain* their original CT parentage. (The mixing of the two CT configurations of the heterodimer will be small due to the substantial energy gap which separates them.) Furthermore, the lowest exciton component of the heterodimer should lie at higher energy than for P in wild-type RCs [22]. From this analysis, the lowest excited state of D can naturally be expected to have more net CT character than the lowest excited state of P. In particular, this CT character would, of course, come from [BChl$^+_{LP}$BPh$^-_{MP}$]. As in our previous discussions [22,23], we believe that the shift to lower energy of this CT configuration, altering (but not eliminating) the mixing of the CT and locally excited configurations, is the key to simultaneously explaining the perturbed long-wavelength absorption of the primary donor and the perturbed primary photochemistry in His$^{M200}$ → Leu RCs compared to wild-type RCs.

Recent low-temperature Stark measurements on *Rb. capsulatus* His$^{M200}$ → Leu RCs [25] and *Rb. sphaeroides* His$^{M202}$ → Leu RCs [36] [†] have resolved two Stark features in the region of the weak near-infrared absorption (840–940 nm) of D. The lower energy feature is observed on the red edge of this band (and in the case of the *Rb. sphaeroides* mutant corresponds to a resolved feature in the low-temperature absorption spectrum). The second Stark feature is found about 1000 cm$^{-1}$ to higher energy. The difference dipole corresponding to the lower Stark feature is found to be in the range 14–43 D for *Rb. capsulatus* [25] and 13–17 D for *Rb. sphaeroides* [36]. The finding of larger values compared to wild-type RCs has led both groups to suggest that the state responsible for the lower Stark feature has more CT character than P*. In agreement with our previous analysis, this has been attributed to a shift to lower energy of the [BChl$^+_{LP}$BPh$^-_{MP}$] intradimer CT configuration in the heterodimer mutant compared to the intradimer CT configurations in wild-type RCs.

The ground state, Stark and transient absorption spectra need to be united in a common framework. An important issue is whether the state we see immediately after a 150 fs flash is the same state that is responsible for the long-wavelength Stark feature. To address this question, we need to know the energy ordering of the lowest excited states of D. Again, these eigenstates are mixtures of the intradimer CT and locally excited configurations of the heterodimer. Hammes et al. [36] have proposed that the lower Stark feature is a state with mostly exciton character (D* in our notation) and place the state with mostly CT character (our D$^\pm$) at higher energy. This proposed ordering of states is the same as is thought to be appropriate for the related excited states of P in wild-type RCs and is the opposite of the ordering we have proposed for the heterodimer mutant (Fig. 2). The proposal by Hammes et al. that D$^\pm$ lies above D* means that the lowest excited state of the heterodimer has at most 50% [BChl$^+_{LP}$BPh$^-_{MP}$] intradimer CT character. However, since we observe a transient with prominent anion absorption character immediately following excitation even at 77 K, it seems clear that D$^\pm$, which we believe has more than 50% (but less than 100%) intradimer CT character, must lie below D*.

Our ordering of the heterodimer excited states is equally consistent with either of two possible interpretations of the Stark measurements: (1) The long-wavelength Stark feature corresponds to D* with the lower energy D$^\pm$ excited state not being resolved in the Stark measurements, due to low oscillator strength and/or being very broad. (The upper Stark feature could then represent vibrational structure in D* [36].) (2) The

---

[†] The primary photochemistry of the *Rb. sphaeroides* His$^{M202}$ → Leu mutant is very similar to that of *Rb. capsulatus* His$^{M200}$ → Leu RCs; McDowell, L.M., Gaul, D., Kirmaier, C., Holten, D. and Schenck, C.C., unpublished results.

lower Stark feature corresponds to $D^{\pm}$, as suggested by DiMagno et al. [25], with the upper Stark feature being due to $D^*$. The ranges of values for the difference dipole and the uncertainty in correlating them with net CT character do not allow conclusive assignment of the lower Stark feature to $D^*$ or $D^{\pm}$. Thus, the extent to which $D^{\pm}$ (the initially observed transient state) contributes to the near-infrared absorption of the heterodimer remains experimentally undetermined. However, the second interpretation is the simplest explanation for all of the available data.

The position of the long-wavelength Stark feature thus places an upper limit of about 1.35 eV on the energy of state $D^{\pm}$. Our measurements show that state $D^+BPh_L^-$ lies below $D^{\pm}$, since the former forms from the latter even at 77 K (see Fig. 2). Since D should be easier to oxidize than P, the free energy of $D^+BPh_L^-$ in $His^{M200} \rightarrow Leu$ RCs is probably somewhat higher than the approx. 1.2 eV free energy of $P^+BPh_L^-$ in wild-type RCs [37–39] [‡]. Thus, our measurements show that $D^{\pm}$ must lie about 1.3 eV above the ground state. This analysis allows us to estimate the free energy of the state in wild-type RCs from which $P^*$ derives its CT character. As described above, this should be a CR state containing substantial contributions from the two intradimer CT configurations of P, whereas $D^{\pm}$ in $His^{M200} \rightarrow Leu$ RCs has mainly $[BChl_{LP}^+BPh_{MP}^-]$ character. Since the two CR states in wild-type RCs will be split in energy from the two intradimer CT configurations, the lower CR component should lie less than 300 meV (the difference in the reduction potential of BChl and BPh in vitro [32,33]) above $D^{\pm}$ in $His^{M200} \rightarrow Leu$ RCs. Therefore, the relevant CR state in wild-type RCs should have an energy of about 1.6 eV or lower, which places it in the vicinity of or lower in energy than the $Q_Y$ states of the monomeric BPhs and BChls and within about 0.2 eV of $P^*$. Won and Friesner [4,10] and DiMagno et al. [25] also suggest that $P^*$ derives its CT character from state that does not lie substantially higher in energy.

*Implications of a dimeric primary donor on charge separation*

To understand fully the optical and dynamical properties of the heterodimer, vibrational and structural relaxations following excitation also need to be considered. Friesner and Won [4] have suggested that the upper vibrational levels of the intradimer CT state $[BChl_{LP}^+BPh_{MP}^-]$ are coupled to the lowest exciton state of D, giving rise to the red-most absorption of D. This implies a fast vibrational relaxation to the zero-point level of $D^{\pm}$ following excitation. It is also very likely that a structural change occurs following excitation of the heterodimer and of P in wild-type RCs. In a strong orbital overlap model, the dimer HOMO is the antibonding combination of the monomer HOMOs and the dimer LUMO is bonding. Thus, excitation should increase the net $\pi$–$\pi$ interaction between the two rings of the dimer, causing them to move closer together [40,41]. (Structural changes within the dimer or the surrounding protein following excitation have been suggested to explain a variety of photophysical properties of P in wild-type RCs [6,8–10,20,40–47].) A decrease in the inter-ring separation would increase the splitting of the two CR states, increasing the net CT character of $P^*$ in wild-type RCs and $D^{\pm}$ in $His^{M200} \rightarrow Leu$ RCs. Interestingly, the decreased distance of charge displacement counterbalances a larger permanent dipole expected from the increased net CT character in the relaxed form of the excited dimer compared to the initially prepared Franck-Condon level. This may explain the observation by Lockhart and Boxer from Stark measurements on wild-type *Rb. sphaeroides* RCs that the difference dipole measured in emission may be slightly smaller than that measured in absorption [48]. A subsequent partial relaxation of the dimer structure may be expected to occur upon electron transfer to $BPh_L$ (wherein an electron is removed from the bonding dimer LUMO but a hole remains in the antibonding HOMO).

Net CT character has consequences not only for the optical properties of the primary electron donor, but for its dynamic behavior and thus the quantum yield of charge separation as well. Our results on $His^{M200} \rightarrow Leu$ RCs at both 285 and 77 K indicate that $D^{\pm}$ has a rapid (about 30 ps) internal conversion (charge recombination) route leading to ground state recovery. Although the CT character of $P^*$ in wild-type RCs is less than that of $D^{\pm}$ in the mutant, it still may be sufficient to endow $P^*$ with an inherent time constant for internal conversion shorter than that of monomeric BChl in solution. (For monomeric BChl the yields of fluores-

---

[‡] The oxidation potential of the heterodimer should be higher than that of P in wild-type because BPh is harder to oxidize than BChl [32,33]. The potential appears to be at least 50 mV higher than that of P (Bylina, E.J., Tiede, D.M. and Youvan, D.C., personal communication), but is probably not 200 mV higher, since the potential would then reach that of monomeric BChl (assuming similar potentials for BChl in vivo and in vitro) and would imply no interaction between the orbitals of the two dimer subunits. (The oxidation potential of strongly-coupled porphyrin dimers is routinely less than the most easily oxidized monomeric subunit [40,54].) In estimating the energy of $D^+BPh_L^-$, the possibility must be considered that the redox potential of $BPh_L$ may be slightly different in $His^{M200} \rightarrow Leu$ RCs than in wild-type, resulting from a secondary change in the RC as a result of the mutation near the dimer. We consider this possibility because of two observations: (i) The time constant for electron transfer from $BPh_L^-$ to $Q_A$ at room temperature is about 100 ps in the mutant compared to about 200 ps in wild-type RCs [22], and (ii) the $BPh_L$ $Q_X$ bleaching in state $D^+BPh_L^-$ (Fig. 1) does not sharpen at 77 K as it does in wild-type RCs. Alternatively, these differences could also reflect an alteration in the distribution of reaction center conformers suggested to be present from recent studies on wild-type *Rb. sphaeroides* RCs [47].

cence, intersystem crossing and internal conversion are roughly 20%, 30% and 50%, respectively, and the singlet lifetime is about 3 ns [49].) At room temperature the quantum yield of $P^+Q_A^-$ (and thus $P^+BPh_L^-$) is 1.02 ± 0.04 [50]; the average P* lifetime is about 3 ps [26,47]; and the fluorescence yield from P* is very low (about $10^{-4}$ [51]). If one takes 0.98 as the quantum yield of $P^+Q_A^-$ (and $P^+BPh_L^-$) formation, then the lifetime of P* in the absence of electron transfer would be about 150 ps. This rough calculation shows that it is easily possible for the internal conversion rate of P* to be an order of magnitude faster than for monomeric BChl and still allow for a near-unity quantum yield of charge separation. Interestingly, the lifetime of P* observed when electron transfer to $BPh_L$ is blocked (by pre-reducing it along with $Q_A$) has been found to be about 20 ps in *Rhodopseudomonas viridis* [52] and about 340 ps in *Rb. sphaeroides* [53]. Despite problems with these measurements (possible reduction of $BPh_M$ and electrochromic effects), the values are of the same order as the estimate just given. Again, this rapid internal conversion rate for P* is likely to be associated with its intradimer CT character.

Although it has been proposed that this CT character may be important in the directionality of electron transfer [6,11,19,20], it is clear from the properties of $D^\pm$ in $His^{M200}$ → Leu RCs that CT character has the disadvantage of providing an enhanced decay pathway that can compete with charge separation. Some CT character in P* may be an unavoidable consequence of overlapping the $\pi$ systems of two macrocycles to make a dimer for other purposes, such as making the primary donor easier to oxidize and shifting the lowest excited state to lower energy to make the RC an effective trap for the excitation in the antenna system. Thus, given a need for a dimeric primary electron donor, the RC may have evolved with a basically symmetrical dimer to limit the net CT character in P* and thus minimize the unwanted internal conversion pathway which degrades the quantum yield of charge separation.

## Summary

We have found that the primary photochemistry in the $His^{M200}$ → Leu RC of *Rb. capsulatus* is essentially the same at 77 and at 285 K. The transient state observed immediately after a near-infrared subpicosecond excitation flash at both temperatures displays a prominant anion band not seen in the P* spectrum of wild-type RCs. We have argued that this transient state ($D^\pm$) has mainly $[BChl_{LP}^+BPh_{MP}^-]$ intradimer CT character. The model we have discussed, with the more exciton-like state D* higher in energy than the more CT-like state $D^\pm$, remains the best explanation for all of the available data. This model provides a framework which unifies the redox potentials of the parent molecules of the heterodimer, the Stark spectrum of the long-wavelength ground state absorption, and the transient absorption spectrum observed shortly after excitation. Our results and analysis suggest that P* in wild-type RCs draws its net CT character from a CR state of the BChl dimer. This CR state lies at higher energy than P* by no more than about 0.2 eV. We also conclude that substantial net CT character in the lowest excited state of the primary donor can significantly reduce the yield of charge separation.

## Acknowledgement

This work was supported by National Science Foundation Grant DMB-8903924. We thank Drs. D. Bocian, S. Boxer and R. Friesner for stimulating discussions, and the authors of Refs. 25 and 36 for copies of manuscripts prior to publication.

## Note added in proof (Received 1 October 1990)

Recently, the results of detailed INDO/S calculations for bacteriochlorin dimers as models for the primary donor P in wild-type RCs have been reported [55]. The authors have stressed the importance of CR states in determining the optical properties of the dimers and how the electronic states will be modified by perturbations such as electric fields. ESR and ENDOR studies on heterodimer mutants have shown that in the oxidized heterodimer the hole is localized primarily on the BChl moiety [56,57].

## References

1 Deisenhofer, J., Epp, O., Miki, K., Huber, R. and Michel, H. (1984) J. Mol. Biol. 180, 385–398.
2 Allen, J.P., Feher, G., Yeates, T.O., Rees, D.C., Deisenhofer, J., Michel, H. and Huber, R. (1986) Proc. Natl. Acad. Sci. USA 83, 8589–8593.
3 Chang, C.-H., Tiede, D., Tang, J., Smith, U., Norris, J. and Schiffer, M. (1986) FEBS Lett. 205, 82–86.
4 Friesner, R.A. and Won, Y. (1989) Biochim. Biophys. Acta 977, 99–122.
5 Parson, W.W. and Warshel, A. (1987) J. Am. Chem. Soc. 109, 6152–6163.
6 Scherer, P.O.J. and Fischer, S.F. (1989) Chem. Phys. 131, 115–127.
7 Meech, S.R., Hoff, A.J. and Wiersma, D.A. (1986) Proc. Natl. Acad. Sci. USA 83, 9464–9468.
8 Boxer, S.G., Middendorf, T.R. and Lockhart, D.J. (1986) FEBS Lett. 200, 237–241.
9 Tang, D., Jankowiak, R., Small, G.J. and Tiede, D.M. (1989) Chem. Phys. 131, 99–113.
10 Won, Y. and Friesner, R.A. (1988) J. Phys. Chem. 92, 2214–2219.
11 Lockhart, D.J. and Boxer, S.G. (1988) Proc. Natl. Acad. Sci. USA 85, 107–111.
12 Lösche, M., Feher, G. and Okamura, M.Y. (1987) Proc. Natl. Acad. Sci. USA 84, 7537–7541.
13 Scherer, P.O.J. and Fischer, S.F. (1986) Chem. Phys. Lett. 131, 153–159.
14 Norris, J.R., Budil, D.E., Gast, P., Chang, C.-H., El-Kabbani, O. and Schiffer, M. (1989) Proc. Natl. Acad. Sci. USA 86, 4335–4339.

15 Dijkman, J.A., den Blanken, H.J. and Hoff, A.J. (1989) Isr. J. Chem. 28, 141–148.

16 Thurnauer, M.C., Katz, J.J. and Norris, J.R. (1975) Proc. Natl. Acad. Sci. USA 72, 3270–3274.

17 Warshel, A., Creighton, S. and Parson, W.W. (1988) J. Phys. Chem. 92, 2692–2701.

18 Won, Y. and Friesner, R.A. (1989) Biochim. Biophys. Acta 935, 9–18.

19 Plato, M., Möbius, K., Michel-Beyerle, M.E., Bixon, M. and Jortner, J. (1988) J. Am. Chem. Soc. 110, 7279–7285.

20 Boxer, S.G., Goldstein, R.A., Lockhart, D.J., Middendorf, T.R. and Takiff, L. (1989) J. Phys. Chem. 93, 8280–8294.

21 Bylina, E.J. and Youvan, D.C. (1988) Proc. Natl. Acad. Sci. USA 85, 7226–7230.

22 Kirmaier, C., Holten, D., Bylina, E.J. and Youvan, D.C. (1988) Proc. Natl. Acad. Sci. USA 85, 7562–7566.

23 Kirmaier, C., Bylina, E.J., Youvan, D.C. and Holten, D. (1989) Chem. Phys. Lett. 159, 251–257.

24 Breton, J., Bylina, E.J. and Youvan, D.C. (1989) Biochemistry 28, 6423–6430.

25 DiMagno, T.J., Bylina, E.J., Angerhofer, A., Youvan, D.C. and Norris, J.R. (1990) Biochemistry 29, 899–907.

26 Kirmaier, C. and Holten, D. (1987) Photosynthesis Res. 13, 225–260.

27 Prince, R.C. and Youvan, D.C. (1987) Biochim. Biophys. Acta 890, 286–291.

28 Holten, D., Gouterman, M., Parson, W.W., Windsor, M.W. and Rockley, M.G. (1976) Photochem. Photobiol. 23, 415–423.

29 Holten, D., Hoganson, C., Windsor, M.W., Schenck, C.C., Parson, W.W., Migus, A., Fork, R.L. and Shank, C.V. (1980) Biochim. Biophys. Acta 592, 461–477.

30 Rodriguez, J., Kirmaier, C. and Holten, D. (1989) J. Am. Chem. Soc. 111, 6500–6506.

31 Gouterman, M., Holten, D. and Lieberman, M. (1977) Chem. Phys. 25, 139–153.

32 Fajer, J., Brune, D.C., Davis, M.S., Forman, A. and Spaulding, L.D. (1975) Proc. Natl. Acad. Sci. USA 72, 4956–4960.

33 Fajer, J., Borg, D.C., Forman, A., Felton, R.H., Dolphin, D. and Vegh, L. (1974) Proc. Natl. Acad. Sci. USA 71, 994–998.

34 Reference deleted

35 Bilsel, O., Rodriguez, J., Holten, D., Girolami, G.S., Milam, S.N. and Suslick, K.S. (1990) J. Am. Chem. Soc. 112, 4075–4077.

36 Hammes, S., Mazzola, L, Boxer, S.G., Gaul, D.F. and Schenck, C.C. (1990) Proc. Natl. Acad. Sci. USA 87, 5682–5686.

37 Woodbury, N.W.T. and Parson, W.W. (1984) Biochim. Biophys. Acta 767, 345–361.

38 Hörber, J.K.H., Göbel, W., Ogrodnik, A., Michel-Beyerle, M.E. and Cogdell, R.J. (1986) FEBS Lett. 198, 273–278.

39 Goldstein, R.A., Takiff, L. and Boxer, S.G. (1988) Biochim. Biophys. Acta 934, 253–263.

40 Duchowski, J.K. and Bocian, D.F. (1990) J. Am. Chem. Soc. 112, 3312–3318.

41 Warshel, A (1980) Proc. Natl. Acad. Sci. USA 77, 3105–3109.

42 Scherer, P.O.J., Fischer, S.F., Hörber, J.K. and Michel-Beyerle, M.E. (1985) in 'Antennas and Reaction Centers of Photosynthetic Bacteria' (Michel-Beyerle, M.E., ed.), pp. 131–137, Springer, Berlin.

43 Kirmaier, C. and Holten, D. (1988) in The Photosynthetic Bacterial Reaction Center: Structure and Dynamics, (Breton, J. and Vermeglio, A., eds.), pp. 219–228, Plenum, New York.

44 Won, Y. and Friesner, R.A. (1988) in The Photosynthetic Bacterial Reaction Center: Structure and Dynamics, (Breton, J. and Vermeglio, A., eds.), pp. 341–349, Plenum, New York.

45 Zgierski, M.Z. (1988) Chem. Phys. Lett. 153, 195–199.

46 Michel-Beyerle, M.E., Bixon, M. and Jortner, J. (1988) Chem. Phys. Lett. 151, 188–195.

47 Kirmaier, C. and Holten, D. (1990) Proc. Natl. Acad. Sci. USA 87, 3552–3556.

48 Lockhart, D.J. and Boxer, S.G. (1988) Chem. Phys. Lett. 144, 243–250.

49 Tait, C.D. and Holten, D. (1983) Photobiochem. Photobiophys. 6, 201–209.

50 Wraight, C.A. and Clayton, R.K. (1973) Biochim. Biophys. Acta 333, 246–260.

51 Zankel, K.L., Reed, D.W. and Clayton, R.K. (1968) Proc. Natl. Acad. Sci. USA 61, 1243–1249.

52 Holten, D., Windsor, M.W., Parson, W.W. and Thornber, J.P. (1978) Biochim. Biophys. Acta 501, 112–126.

53 Schenck, C.C., Parson, W.W., Holten, D. and Windsor, M.W. (1981) Biochim. Biophys. Acta 635, 383–392.

54 Buchler, J.W., De Cian, A., Fischer, J., Hammerschmitt, P., Löffler, J., Scharbert, B. and Weiss, R. (1989) Chem. Ber. 122, 2219–2228.

55 Thompson, M.A., Zerner, M.C. and Fajer, J. (1990) J. Phys. Chem. 94, 3820–3828.

56 Bylina, E.J., Kolaczkowski, S.V., Norris, J.R. and Youvan, D.C. (1990) Biochemistry 29, 6203–6210.

57 Huber, M., Lous, E.J., Isaacson, R.A. Feher, G., Gaul, D. and Schenck, C.C. (1990) in Proceedings of the Feldafing Workshop on the Structure and Function of Bacterial Reaction Centers (Michel-Beyerle, M.E., ed.), Springer, Berlin, in press.